NEUTRON ACTIVATION ANALYSIS USING MONOENERGETIC GAMMA-RAY SPECTRA

by

E. Larry Robinson

Thesis submitted to the Graduate Faculty of the

Virginia Polytechnic Institute

in partial fulfillment of the requirements for the degree of

DOCTOR OF PHILOSOPHY

in

Physics

APPROVED:

Dr. A. K. Furr, Chairman

Dr. R. L. Bowden

Dr. A. Robeson

Dr. R. F. Tipsword

Dr. J. A. Jacobs

August, 1969

Blacksburg, Virginia

ACKNOWLEDGEMENTS

The author wishes to thank the members of his committee, Dr. James A. Jacobs, Dr. Andrew Robeson, Dr. Robert L. Bowden, and Dr. Ray F. Tipsword, for serving in that capacity. Special thanks are extended to Dr. A. Keith Furr for serving as the author's research advisor. Dr. Furr was always available for discussions and offered numerous valuable suggestions during the course of this work.

The author would also like to acknowledge the help of fellow graduate students, Messrs. Wayne Campbell, Gordon Lindsay, and Elias Stergakos, for helpful discussions and reactor operation. The author also appreciates the help of Miss Jo Collier in preparing numerous graphs.

To his wife, Joyce, the author expresses his sincere thanks for the understanding and encouragement offered throughout his academic career.

The author would like to acknowledge the financial assistance provided by the Atomic Energy Commission in the form of a Traineeship under which part of this work was carried out.

TABLE OF CONTENTS

LIST OF FIGURES

LIST OF TABLES

INTRODUCTION

When one wishes to determine the constituents of a sample, he has the task of choosing an applicable method from a great many possibilities. There are many choices including spectrographic techniques, mass spectroscopy, a host of chemical methods (gravimetric tests, colorimetric tests, and many other chemical determinations), and, as will be discussed in this work, neutron activation analysis. One would like the analysis to be accurate, precise, nondestructive, fast, and universally applicable. While no single procedure can satisfy all the above requirements, many of the above methods are flexible, useful, and are widely employed.

Over the past 30 years, from its beginning[5] not long after the discovery of the neutron, activation analysis has progressed to the point of being close to satisfying most of the above criteria. The technique is well suited for a wide variety of elements, because of its sensitivity which is often much higher than any other method, by an order of magnitude or more. For elements for which the sensitivity to neutron activation analysis is low, quantities in the 1-10 μg region may be determined. For ultra-sensitive elements the range can be as low as 10^{-6} to 10^{-7} μg. The detection level for a median sensitivity element would be about 0.001 μg. Some 75 elements may be detected in the interference-free limits given above[1]. While each experimental facility would have its own limitations due to the locally available neutron source and counting equipment, the results quoted above provide an indication of the extreme usefulness of the neutron

activation analysis technique.

In this technique, the constituents of a sample are inferred from the characteristics of the induced radiation emitted by the product nuclei formed upon bombarding the sample with neutrons. The data to be analyzed usually consist of spectra, accumulated in a storage unit such as a multichannel analyzer, which represent the number of detected events as a function of energy deposited in a detector. This detector is usually either a NaI(Tl) scintillation crystal mounted on a photomultiplier tube or a solid-state device such as a lithium drifted germanium diode. In a typical system, the data are stored in 200 or more channels in the storage unit. In most cases, the analysis is based on the recognition of photoelectric events within the detector resulting from gamma rays from the sample since these correspond to definite peaks in the data. Other types of interactions result in broader and less identifiable features in the accumulated data. Analysis of the data can be done by hand but, if a large number of spectra, which sometimes are necessary for analysis of a single sample, are involved, it is obvious that this method quickly becomes unreasonable. Large numbers of computer programs have been written which would permit ready analysis of large numbers of spectra. Most of these programs have an inherent fault in that virtually all of them presuppose a knowledge of the constituents and compare the data for an "unknown" sample with the proper spectra for the expected constituents. Obviously, if the proper constituents for comparison are not chosen, then all of the elements present within a specimen will not be identified, and in the case of many of these programs, a component of the sample specimen will be erroneously identified.

Thus, ideally, it would be desirable to have every conceivable standard spectrum stored in one's computer and available for comparison. In certain simple cases where repeated measurements on similar samples are involved with only a few possible contributors to the data, such as in many industrial applications[3,4] such an approach is quite feasible and is widely employed. In general, however, such an approach will lead to an enormous, unwieldy library.

In an effort to reduce the size of the needed library, a completely different approach was tried by Robins et al.[22] They assumed that any complex gamma ray spectrum resulting from several gammas from the sample was made up of the superposition of the effects caused by the individual gammas present. Thus, instead of a large library of all possible isotopic spectra, it should in theory be possible to store a library of the response of the detector system to monoenergetic gammas and build up a composite from these spectra for any more complex spectrum. Fortunately, the response of the detector to gammas of different energy is not a strong function of energy so that it is not necessary to have a library monoenergetic gamma of precisely the same energy as another for the comparison to be possible. Robins et al. showed that, over the gamma energy range of about 0.2 - 3.1 meV, approximately 30 monoenergetic gamma spectra were sufficient to satisfactorily fit any gamma ray in this energy region. With few exceptions, the presence of a given element for which neutron activation analysis is suitable, can be ascertained by the presence of a gamma in this energy range.

Although the concept of a relatively small library of monoenergetic gammas was adequately demonstrated, there were two major deficiencies in

the original program. The form of the program required nearly perfect data to function and no quantitative results were provided. It is the purpose of this work to remedy both deficiencies.

Numerous specific uses for neutron activation analysis have appeared in the literature; for example, references 12, 13, and 14 are representative of the current literature. Selected lists of references are available[9,10] as well as textbooks and handbooks[6,7,8,16]. There is even an excellent introduction at the popular level[2].

Systematics and Criteria

The target may be irradiated using either thermal or fast neutrons and the induced radiation may differ markedly because the specific reaction involved could depend on the incident neutron energy. However, for the moment, let us restrict our concern to the analysis of the induced radiation after the activation without regard to the original mechanism by which it was produced. It will be necessary to consider this factor when identification of a specific precurser is required, but most of the program does not depend in any way on the manner in which the activity arose in the sample.

A simple detector system is shown in Figure 1 and consists of a detector which transforms the energy of the incident gamma into an analagous voltage or current pulse, an amplifier (which may include a preamplifier) to increase the amplitude of the signal and a storage unit. The latter is usually a small fixed-program computer with an analogue to digital converter in the input which digitizes the analogue pulse and stores it in a memory location appropriate to the size of the pulse. The spectra referred to earlier represent the cumulative storage of thousands of such pulses representing the decay and detection of the emitted radiations of thousands of individual nuclei in the sample.

Each of the components of the counting system affect the stored data in different ways. Although lithium drifted detectors are rapidly coming into favor,[17] their low sensitivity relative to NaI(Tl) detectors usually reduces the sensitivity of the method by an order of magnitude or more. Thus, we will restrict ourselves in the remainder of this

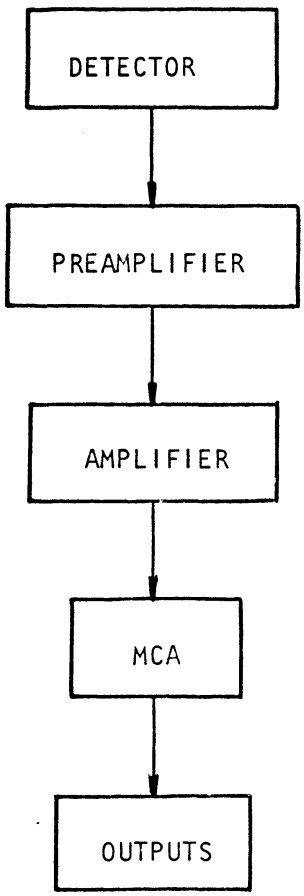

Figure 1. Typical Single-Detector Counting System

section to consideration of a NaI(Tl) detector system.

The interaction of a gamma ray with the detector crystal results in light being emitted which then results in a response by the photomultiplier tube to which the crystal is attached. Because of the nature of the interaction, the detector introduces a considerable spread in the resulting pulses for a specific process occurring in the crystal. For example, in a typical system interactions of 0.662 meV gammas from ^{137}Cs which leads to a photoelectric event results not in a single line in a spectrum but rather a Gaussian shaped distribution with a half width of 6-7% of the photon energy. Not all the interactions are photoelectric events, however, and the resulting spectrum is even more complex than this single broadened line[11].

Each of the other components affect the resulting stored data, although none as drastically as the detector itself. For example, very high counting rates result in the gain of the photomultiplier shifting relative to that at low counting rates. The multichannel analyzer requires a finite time to store a single event and will not record all the data when it arrives too rapidly. The resolving time of the system is finite and when pulses arrive at such a rate that more than one pulse falls within the resolving time of the detector, the photomultiplier or the amplifier, they are treated as a single pulse with a consequent distortion of the stored data. Thus, a compromise is necessary between the desire for a high counting rate so that data may be acquired rapidly and the errors introduced by too rapid a counting rate. It has been determined that little error is introduced by the remaining components in the system if the analyzer in use in the V.P.I. system does not

exhibit a dead or busy time greater than about 10%.

If we refer to Figure 2, we see the stored spectrum for a radioactive sample of ^{28}Al made by the capture of a neutron in natural aluminum. This is a monoenergetic gamma emitter and was used in compilation of the library spectra. It exhibits all of the features to be expected in a single gamma spectrum. The peak at the upper end (channel 172) corresponds to a photoelectric interaction of the 1.78 meV ^{28}Al gamma. The full width at half-maximum of the distribution is about 5%. Earlier, it was mentioned that for a similar peak at 0.662 meV, a typical system would have a width of about 7%. The resolution of a system does improve with increasing energy and, conversely, becomes much worse at very low energy. Over the range just mentioned it can be seen that the resolution does not change rapidly with energy. Hence, shifting a photopeak a few channels (in order to make one spectrum match another) would not appreciably distort the shape of the peak. It is also found that if one fits a Gaussian distribution to the photopeak, that it is a good approximation to the peak and could be employed to represent it.

Below the photopeak area, a broad general plateau (ignoring small bumps) exists due to Compton scattering of the incident gammas. The cross section for this process peaks at forward scattering of the target electron so that this distribution reaches a maximum at its highest energy. The number of scattered gammas due to the forward scattered electrons are also maximized and the scattered gammas retain the minimum amount of energy possible. Thus, these gammas scattered at

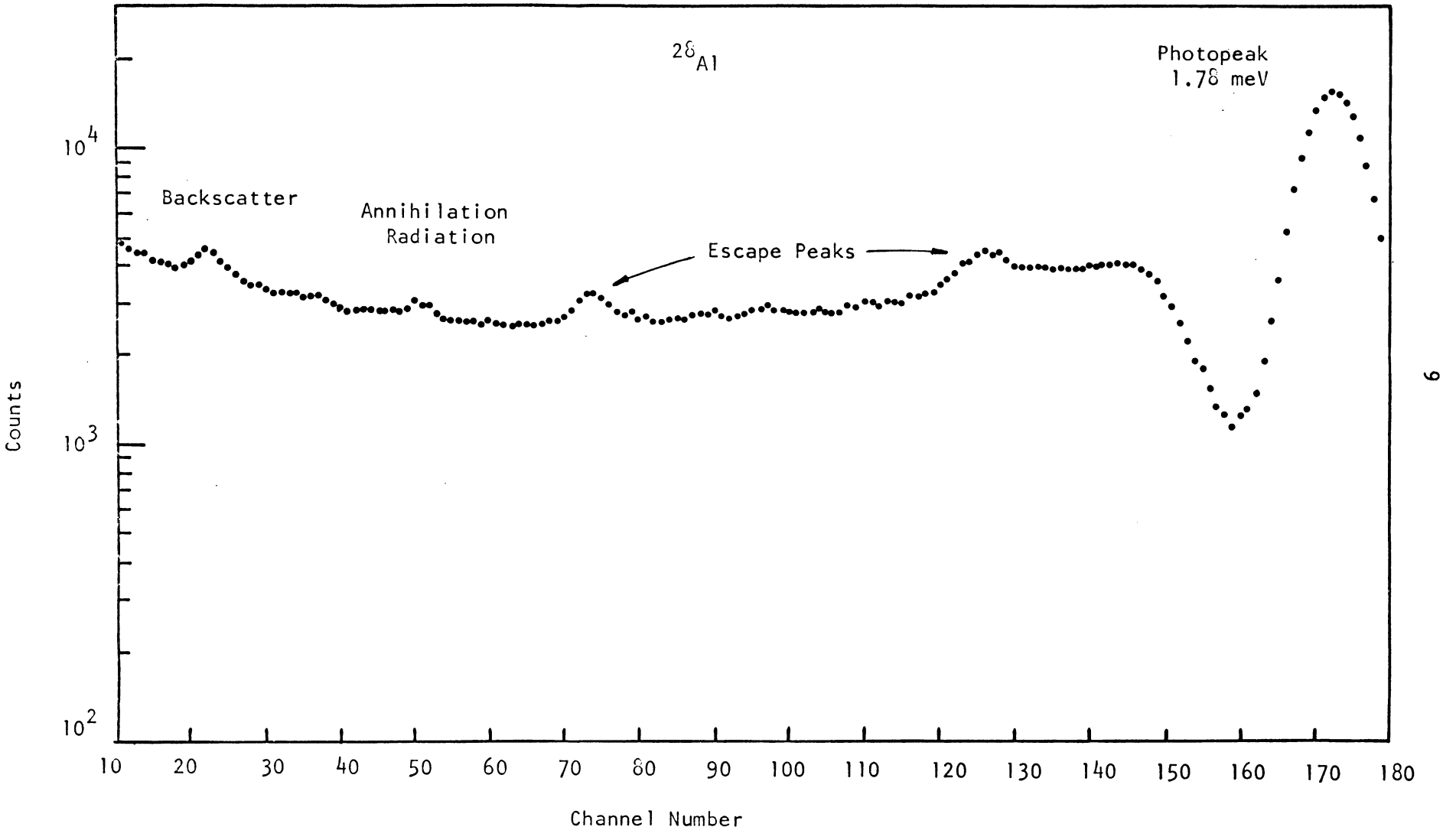

Figure 2. Example of Data Accumulated by a Multichannel Analyzer

180^{o} with respect to the incident gamma give rise to a "back-scatter" peak in the distribution.

For a gamma above 1.02 meV, pair production is possible. Thus, we have events associated with this process. The two escape peaks in the figure correspond to escape of either one or both of the annihilation gammas created when the positron combines with an electron in the detector crystal. The annihilation peak is the 0.511 gamma caused by the detection of one of the two annihilation gammas resulting from an interaction in the surrounding structure.

A similar distribution would be found for any monoenergetic gamma and the library consists of a compilation of approximately 30 of these distributions concentrated in the first 100 channels. Above this point, the number of gammas occuring in samples becomes fewer and the library distributions are selected to reflect this fact. However, the relative size and shape of the various components vary with energy. As already indicated, the pair-production process only occurs above 1.02 meV and is actually not important until well above this minimum energy.

The cross section for a photoelectric event increases rapidly with decreasing energy as shown later in the section on quantitative measurements while the cross section for a Compton event increases much more slowly. The result of the combined variation of these two factors is that the ratio of the area under the photopeak to the total number of events in the spectrum varies from 12% at the high energy end of the spectrum to nearly 75% at the low end. Since there are 200 data channels in the present system,[19] this corresponds to approximately a

variation of approximately only 0.3% per channel. As will be discussed in the section dealing with the actual program, a shift of a library spectrum is limited to a maximum of 2 channels and in the huge majority of cases, the shift will be much less. Actual tests, performed by Robins et al. who checked the senstivity of the system to the variables affecting the shape of the distributions, using shifts of the magnitude just cited, show that the major variation in the photofraction data is due to the lowest channels. Since the program is expected to perform poorly in these channels and is usually restricted to gammas above about 200 keV, the variation in the shapes of nearby peaks is actually expected to be even less than would be indicated by the photofraction data cited above.

Another way of appreciating the degree of variation to be expected between a shifted peak and an actual peak at the same location is to compare the resolution of the system and the energy differential corresponding to the shift. The calibration of the system is such that one channel represents an energy spread of about 15 keV so that the maximum shift permitted is about 30 keV. The system resolution is generally larger than this. At the two energies cited earlier, 0.662 for ^{137}Cs and 1.78 meV for ^{28}Al the actual energy resolution of the system is 47 keV and 90 keV respectively. Thus, the maximum shift is within the range where the system could readily distinguish between the two gammas.

Not all the monoenergetic gammas employed were obtained directly by activation of a specific target nuclide, but were obtained by interpolation between two close measured gammas. An examination of the interpolation routine was carried out by interpolating a gamma for which

an actual one was available for comparison. Even when the two gammas employed for interpolation were 15 to 20 channels apart, errors of total areas and peak areas were on the order of 1%, with again the largest error at the bottom of the Compton distribution. This again, indirectly, serves to substantiate the contention that small shifts of a library spectrum to match an actual photopeak leads to negligibly small errors.

The data were smoothed prior to an analysis using a Gaussian filtering technique which essentially examined all the data in the region of a data point to ascertain whether a deviation from the surrounding data points was real or not, and if due only to statistical fluctuations, reduced the deviation. This step is not altogether necessary but does serve to reduce to an extent the number of false low statistics peaks to be analyzed. In order to further eliminate the number of low count rate apparent peaks which the program might try to analyze, a minimum count rate test was included. The level of this criteria can be varied such that the level is small compared to the average data. Normally, an arbitrarily selected value of 100 counts/channel is employed which has proven generally satisfactory.

One of the most serious problems associated with the spectrum stripping technique is the matching of the exact centroids of the library photopeaks and the photopeak being examined. The areas between the points on either side of the photopeaks corresponding to half-maximum are least square fitted to a Gaussian distribution as indicated earlier. The centroids of both the library photopeak and specimen peaks are matched to within a tenth of a channel. A looser criteria was found to result in areas on either side of the center of the specimen gamma

where the peak was either under or over subtracted and in extreme cases, the program could attempt to analyze the under subtracted points as an additional peak.

It was found that properly matching the photopeak areas and then subtracting the entire distribution is adequate and normally leaves a nearly random number of positive and negative residuals. If the library peak is shifted downward, then, because the photofraction for the library gamma is lower than it should be, a few more channels will be negative in the Compton distribution area than should be, while if the library spectrum is shifted upward, the opposite is true. Otherwise, the concept of employing a monoenergetic library to reduce a complex gamma ray spectrum has been shown to lead to extremely small errors, and unless a large number of library spectra are successively subtracted from the same area, even this effect is negligible.

Since beta radiation is prevented from entering the detector system by the presence of a carbon beta absorber between the source and the detector, it would appear from the above discussion that it should be possible to selectively strip all contributing gamma spectra from any complex spectrum using the stored library. In a very large number of cases, this is true but in a few cases an additional complication is present. In the decay of some radioisotopes such as ^{31}Si, where a single monoenergetic gamma 1.27 meV gamma is emitted, the emitted radiation is masked by strong bremstrahlung emission from the radioactive isotope. In the case cited, the bremstrahlung spectrum extends to above 1.48 meV and completely distorts the normal gamma ray spectrum.

In such cases, which fortunately are not numerous, it would be very difficult to use a scheme as is employed in the present program and one would be forced to use the specific spectrum for the specific isotope in a computer program.

COMPUTER PROGRAM

At the beginning of the present investigation a computer program had been developed at VPI for performing qualitative neutron activation analysis. Various stages of the development are described in references 20, 21 and 22. The technique involved some novel features including the use of monoenergetic gamma-ray spectra instead of the usual isotopic spectra. The procedure required a minimum of input data (e.g., neither the positions of the photopeaks nor initial estimates of the constituents was required). The program did, however, impose stringent conditions on the consistancy of the data as the analysis was being carried out.

The goals of the present work were two. First, a modification of the program then in use was sought so that as much information as possible could be extracted from a set of data even in the case in which difficulties were encountered during the computer analysis. The second goal was to extend the computer analytical program to include quantitative results. In carrying out the first of these aims, that of making the qualitative analysis more flexible, an effectively new program was developed.

Several of the basic features of the old program were retained. The qualitative analysis is still effected using the spectrum stripping technique. Also, the library of monoenergetic gamma-ray spectra was retained. However, the way in which the data are analyzed within the framework of the spectrum stripping technique has been substantially altered. These modifications to the qualitative analysis and the

extension to quantitative analysis will be described in more detail below.

Qualitative Analysis

Figure 3 is a block diagram which gives the major features of the new program. The library of monoenergetic gamma-rays and the experimental data (up to ten spectra) are read into the computer. The experimental data is then smoothed before the analysis begins. The smoothing procedure has been described in reference (20).

One of the major disadvantages of the old program was that only two estimates of the half-life of a given peak were obtained. Since only two estimates were calculated, and the resulting average half-life was used to extrapolate back in time to strip the given photopeak from all spectra, the analysis was terminated if the upper and lower confidence limits (corresponding to the 95% probability level) of the two estimates did not overlap. This rather stringent requirement was necessary since such a stripping could affect all the data. Another disadvantage of this treatment of the data was that the normalization of the library spectrum to a single photopeak could affect every spectrum. In the old program after a photopeak had been located and verified by statistical tests in the n^{th} spectrum the corresponding peak in the preceeding or $(n-1)^{st}$ spectrum was sought. However, it often happened that the most energetic peak in the $(n-1)^{st}$ spectrum did not correspond to the peak in question. This situation necessitated the temporary stripping out of all peaks above the desired photopeak. These peaks were added back in after the

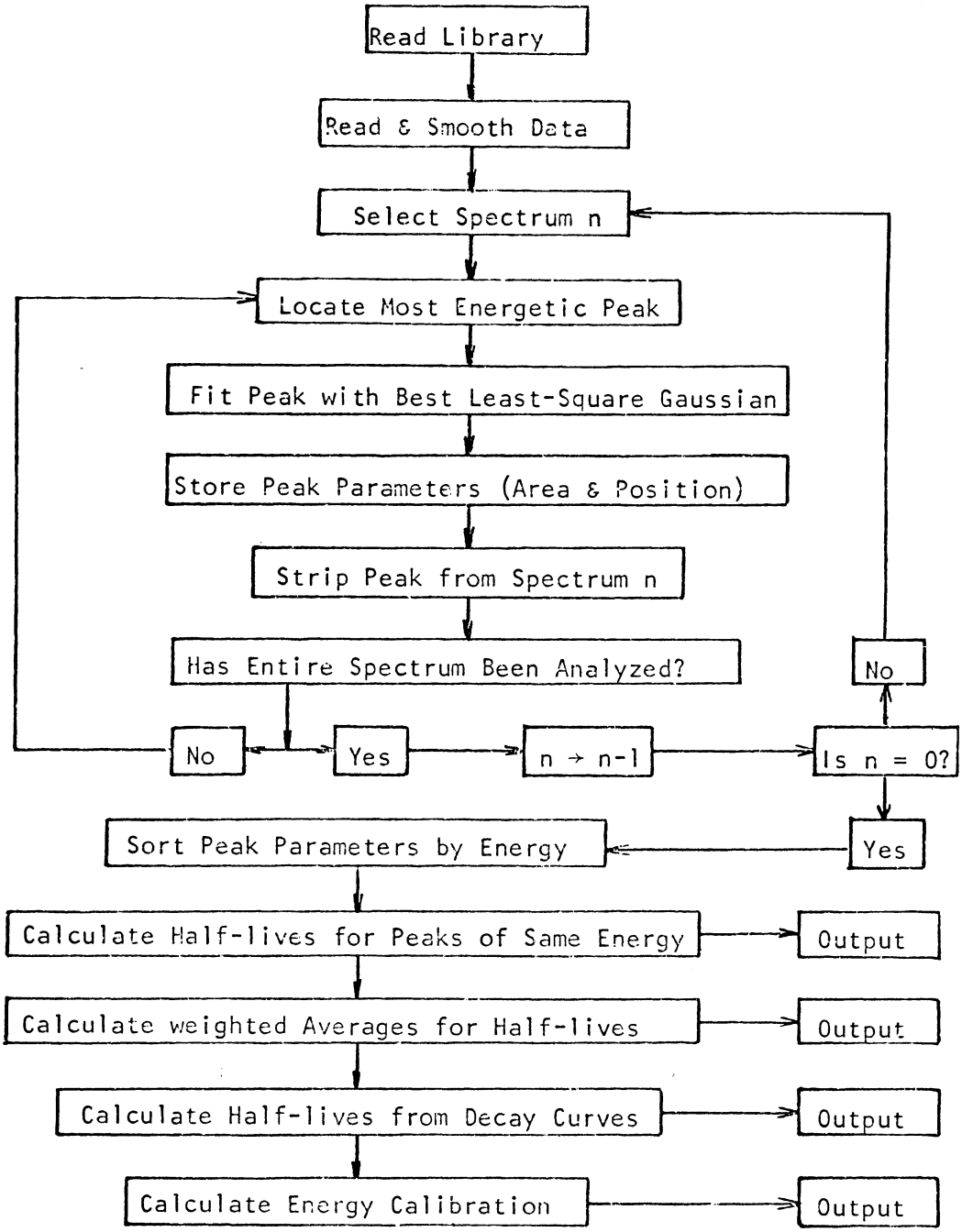

Figure 3. Block diagram showing major features of new qualitative analysis computer program.

necessary tests and calculations had been performed. Before a peak could be satisfactorily stripped out, the peak had to be located and verified statistically and fitted with a best least-square Gaussian function. The last step (the fitting procedure) was necessary because whether a stripping was satisfactory depended very greatly on knowing the exact centroid of the photopeak. Thus, a good deal of extra work often had to be performed just in order to obtain an estimate of the half-life. The same situation, that of performing extra work, occurred once the average half-life had been obtained, i.e. during the extrapolation back in time and stripping out of the monoenergetic spectrum, higher energy peaks than the one in question were routinely present. These peaks also had to be temporarily removed before stripping out the peak under analysis could be performed.

The new program avoids the extra work and computer time by analyzing each spectrum separately. The analysis is carried out as indicated in Figure 3. The most energetic photopeak of a given spectrum is located and verified. The peak is then fitted by a best least-square Gaussian function. The location (non-integer channel number) of the centroid and the area under the peak, i.e. the sum of the channel counts in the photopeak, are obtained from the fitting procedure and are stored for future use. The appropriate library spectrum is then selected, normalized, and used to strip out the photopeak under analysis. This stripping is carried out only in the spectrum under analysis. The program then moves to the next most energetic photopeak in that spectrum and the above steps are repeated. This procedure continues until all the peaks are removed from that

spectrum. Each spectrum is analyzed in turn in the same manner.

Thus a spectrum consisting of 200 data points is reduced to two sets of parameters, the peak positions and peak areas of all photopeaks present in that spectrum. The calculation of the estimates of the half-lives uses the peak areas since this is considered to be the most accurate estimate[23].

Once all spectra have been analyzed to yield peak positions and areas, these parameters are sorted into groups. Each group consists of those peaks with the same peak position or energy. The activity due to each photopeak is then calculated using the peak area and appropriate counting time. The half-life estimates along with confidence limits are calculated from the activity data. If m estimates of the activity due to a given photopeak are known then the number of estimates of the half-life is

$$\text{number of estimates} = \frac{m!}{2!\ (m-2)\ !}$$

i.e. the number of combinations of m activities taken two at a time. For example, if eight spectra are taken and a given photopeak occurs in all eight spectra, then one obtains 28 estimates of the half-life.

The mean of the calculated half-lives and confidence limits is computed. Each set of confidence limits is then compared to the mean confidence limits, and when the limits do not overlap, that half-life and limits are rejected. Those remaining are used to calculate a weighted average half-life and confidence limits. The weighting factor for each estimate is based on the peak areas used in calculating the half-life.

A comparison of the two versions of the computer program in estimating half-lives in a test case[22] are shown in Table I. It is obvious that the new procedure gives significantly better estimates.

In addition to the weighted average half-life and limits described above, an estimate of the half-life which can be compared with the weighted average is obtained from a least-square line fit to the logarithim of the activity versus time plot of all the activity data points.

The new method of computing the half-lives has another advantage in addition to obtaining many more estimates than the old procedure. It is possible that more than one radioisotope is contributing to a particular photopeak. For example, if ^{65}Ni which emits a gamma-ray of 1.49 MeV and ^{42}K which emits a gamma-ray of 1.52 MeV are both present in a sample, then an apparent photopeak would appear at about 1.51 MeV. This apparent photopeak would decay with a changing half-life since the actual half-lives are 2.56 hours and 12.4 hours respectively. In the present method of analysis one could observe the change in the calculated half-life as a function of time, and perhaps be able to extract both half-lives.

Thus, the new procedure has distinct advantages over the old procedure. Each photopeak in an individual spectrum needs to be analyzed only once, and the stripping is no longer based on extrapolation in time with an imperfectly known half-life. Ironically, the old procedure was originally chosen to reduce the work required in the analysis. However, problems were encountered which necessitated a vast increase in the work and computer time, as described previously.

TABLE I

Radionuclide	Photopeak Energy (MeV)	Half-Life		
		Actual	Old Program	New Program
^{64}Cu	0.511	12.8 h	13.2 ± 1.3 h	12.6 ± 1.3 h
^{66}Cu	1.04	5.1 m	5.4 ± 0.5 m	5.2 ± 0.5 m
^{64}Cu	1.34	12.8 h	13.7 ± 3.7 h	12.2 ± 1.5 h
^{28}Al	1.78	2.3 m	2.3 ± 0.1 m	2.3 ± 0.4 m

Another of the many changes is the way in which a library spectrum is normalized for the subtraction of a photopeak. In the old program a specified number of channels (varied with energy of photopeak) above and below the peak channel were summed. The library spectrum chosen for the stripping underwent the same procedure. The normalization constant was then defined as the ratio of these two sums. In the new program, after the library spectrum has been gain shifted, the library spectrum is normalized so as to make it a best least-square fit in the channels between the half-maxima on either side of the peak. Also, previously the above sum over the data peak was used in the half-life calculations, whereas now the area of the fitted Gaussian function is employed.

A new feature of the qualitative analysis is that the energy calibration for a given set of data is calculated. A calibration spectrum consisting of ^{60}Co and ^{137}Cs is taken just before the data is accumulated. The gain of the counting system may change in time due to temperature change or high counting rates. This possibility of gain shift is acknowledged by allowing the peak position to vary by $\pm$ 2 channels ($\sim \pm$ 30 keV) in the sorting process. The three gamma-rays in the calibration source are fitted with a best least-square line to yield the calibration curve (the energy response of NaI(Tl) in the typical energy region of interest, about 0.2 MeV to about 3.1 MeV, can be considered linear for purpose of calculation). The mean peak position of a series of corresponding peaks in the data is used to calculate the energy of that series using the fitted line.

In summary, the present qualitative analysis program differs markedly from the old. The results which one obtains from the program are the mean energies and the weighted half-lives of corresponding photopeaks. In order that one may get an indication of the reliability of the results, the activity and associated time for each series of peaks is also part of the output. By plotting the logarithim of the activity versus time, one can judge whether a single decay is present, whether more than one decay is present, or whether no reliable conclusions can be drawn. The half-life obtained by fitting this curve is also available as indicated previously. As a further aid in helping one decide what isotopes are present in the sample the relative intensity of the peaks within a given spectrum are also presented. This relative intensity, obtained by dividing the peak area by the absolute peak efficiency, would be useful when the half-life results indicate that two or more peaks have the same apparent half-life. This gives one three parameters from which assignment of isotopes present can be made. Also, additional data are presented so that one may perform the quantitive analysis with a minimum of hand calculations if desired. This feature will be described in greater detail in the following section.

The results of the new program have already been compared with that of the old qualitative analysis program. Another test case will be presented in a later section, and examples of the output described above will be shown.

Quantitative Analysis

Quantitative activation analysis is difficult whether one uses the absolute calibration technique or the comparator technique (these techniques will be described below). The former method is difficult because of uncertainty in the cross-sections and the possibility that the flux can vary during activation. Differences in the physical characteristics of the sample and the comparator can lead to errors in the latter method. Thus, in the development of the quantitative aspect of the present work, a wide latitude in the possible methods of analysis was built into the program. While absolute calibration of the counting system with corresponding analysis is more consistant with the method of qualitative analysis used, other possibilities have not been ignored, and a flexible quantitative analysis computer program has been developed.

Comparator Technique

In this method a known weight of a pure sample containing the specific element is activated with the unknown sample. Since the two samples are activated together the irradiation time and flux are the same for both samples. The following simple equation is then applicable:

$$\frac{W_x}{W_s} = \frac{A_x}{A_s}$$

where

W_x = weight of unknown

W_s = weight of standard

A_x = disintegration rate of unknown

A_s = disintegration rate of standard

If ε represents the overall efficiency of the counting system, then the following relations can be used.

$$R_x = \varepsilon_x A_x$$

$$R_s = \varepsilon_s A_s$$

where

R_x = counting rate of unknown

R_s = counting rate of standard

ε's = the respective efficiencies

Thus, we have

$$W_x = \frac{W_s R_x \varepsilon_x}{R_s \varepsilon_s} = \frac{W_s R_x}{R_s} \quad .$$

The last equality holds if $\varepsilon_x = \varepsilon_s$. This relation is true if one chooses the correct standard.

As stated before differences in the physical characteristics of the sample and comparator can lead to erroneous results. For example, the thermal flux can be enhanced by moderation of epithermal neutrons by light nuclides present in the compounds employed.

This technique is obviously very useful when one wishes to determine the quantity of some particular element present in a sample. Also obvious is the fact that if one does not pick the proper comparators, very serious errors will be encountered since it would

be unlikely for the efficiencies to be the same.

Absolute Calibration

When N atoms of an isotope with an activation cross-section of σ, are irradiated in a reactor having a neutron flux ϕ for a period of time t, the induced activity at the end of irradiation of the product isotope (assumed radioactive with decay constant λ) is given by

$$A = N \sigma \phi (1 - e^{-\lambda t}) \quad .$$

One does not usually determine the activity directly. However, as used in the previous section the measured counting rate is proportional to the activity, i.e.

$$R = \varepsilon A$$

where

R = measured counting rate

ε = overall efficiency

If the counting rate is based on the photopeak, then $\varepsilon = \varepsilon_p$. The quantity ε_p is defined as the probability that a gamma-ray of energy E emitted from the source, will appear in the photopeak of the observed pulse-height spectrum. The quantity as defined here is the overall efficiency for the photopeak, including the solid angle subtended by the detector. The basic equation then becomes

$$R = N \sigma \phi \varepsilon_p (1 - e^{-\lambda t}) \quad .$$

Incident beta particles can almost completely obscure the desired gamma-ray spectrum. Therefore, a beta absorber (a one centimenter

thick piece of graphite in the present case) is used to reduce the number of beta particles entering the detector. This beta shield also affects the gamma-ray spectrum as shown in Figure 4 for the photopeak events. The figure shows the ratio of the peak area with the shield in place to the area without the shield as a function of energy. Let this correction be denoted as A, and the equation becomes, with the factor included,

$$R = N \sigma \phi \varepsilon_p A (1 - e^{-\lambda t}) \quad .$$

The factor ε_p is, of course, energy dependent. If one wishes to use the above procedure, one needs to determine ε_p and ϕ, or equivalently the product $\phi\varepsilon_p$.

The function $\varepsilon_p(E)$ is difficult to obtain, although methods exist for its determination[24]. The usual procedure is to use the calculated values of ε_t which is the probability that a gamma-ray of energy E emitted from the source, will cause some interaction and appear in the observed pulse-height spectrum. The two quantities ε_p and ε_t are related as follows

$$P = \varepsilon_p/\varepsilon_t$$

where

P = photofraction or peak-to-total ratio.

The photofraction is the ratio of the sum of the counts in the photopeak to the sum of the counts in the entire pulse-height distribution. The photofraction can be measured without too much difficulty. The measured photofraction data for the V.P.I. system are shown in Figure 5. This

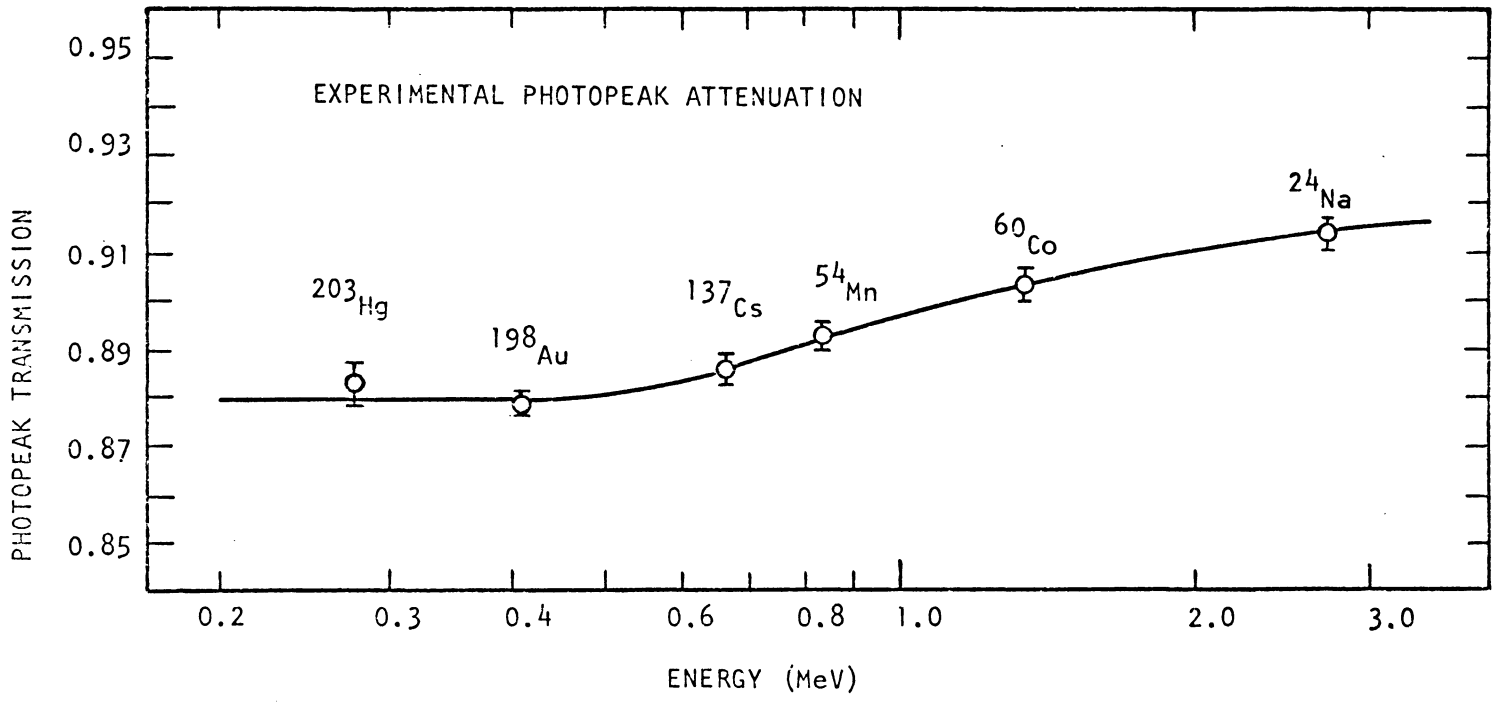

Figure 4. Experimental Photopeak Attenuation due to the Beta Shield.

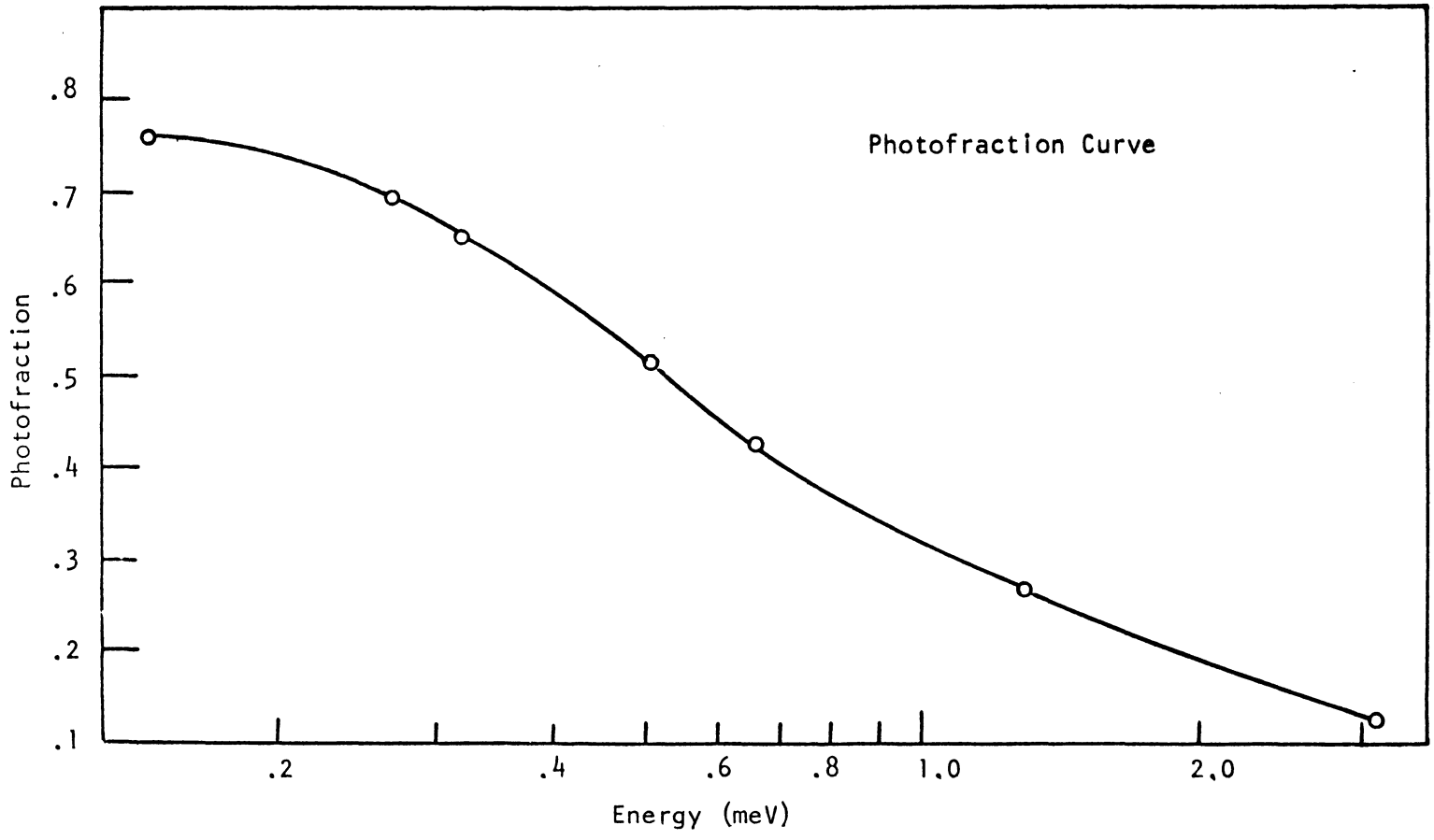

Figure 5. Experimental Photofraction Curve. The Errors Associated with the Experimental Points are of the Order of the Circle Diameters.

curve and the appropriate ε_t calculations taken from Heath[25] were used with the equation above to obtain the relative ε_p as a function of energy. The resulting curve is shown in Figure 6.

Rather than determining the absolute ε_p curve, the absolute product $\phi\varepsilon_p$ was determined using the nuclides ^{27}Al and ^{197}Au. These nuclides were activated at the rabbit site in the V.P.I. reactor. The results of this calibration multiplied by the photopeak attenuation are shown in Figure 7.

In order to use this data with the activation equation to determine quantities of elements present in a sample, the areas of the photopeaks present in the experimental data are needed. Thus, some fitting procedure is required.

Fitting Procedures

One of the standard fitting procedures used is that of least-squares. The basic problem is the following: given an experimental spectrum or array of numbers and given a known set (from the qualitative analysis) of spectra, what is the proper linear combination of the members of the set so that the sum of the squares of the differences between the experimental spectrum and the linear combination is a minimum. This is a standard least-squares problem and has been discussed in many sources, e.g. reference (26).

The problem can be formulated as follows. Let ρ_i represent the number of counts in channel i of an experimental spectrum. Assuming there are m components in the experimental spectrum

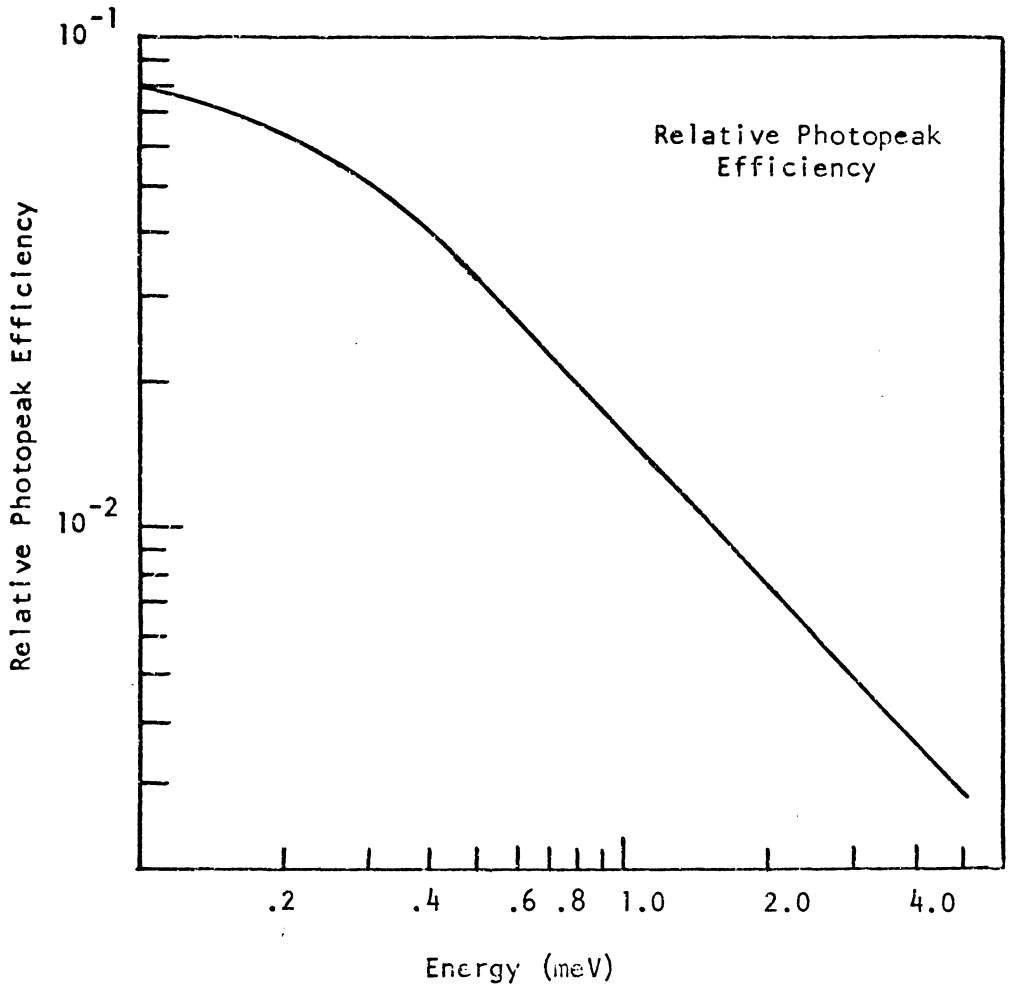

Figure 6. Relative Photopeak Efficiency. This Curve was Obtained by Multiplying Point by Point the Relative Efficiency Times the Photofraction.

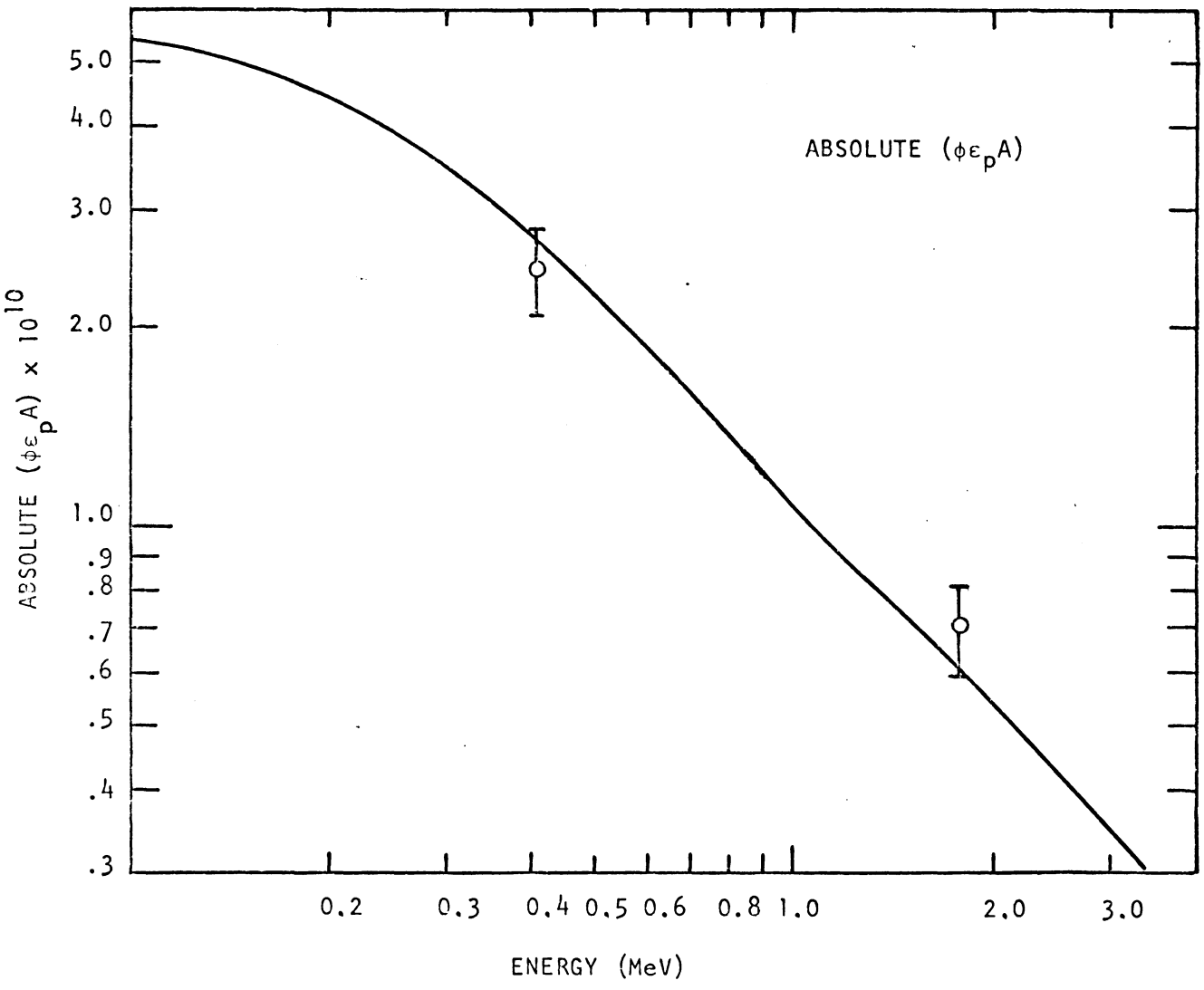

Figure 7. Results of Normalization of the $\varepsilon_p\phi$ Curve. This Result has also been Multiplied by the Photopeak ^{p}Attenuation A.

$$\rho_i = \sum_{n=1}^{m} B_{in}$$

where B_{in} is the count in channel i due to the n^{th} component. If, however, the components of the experimental spectrum are known but the intensities of the components are not known, then

$$\rho_i = \sum_{n=1}^{m} \beta_n A_{in}$$

where β_n represents the normalizing factor for the n^{th} array A_{in}.

$$\beta_n = B_{in}/A_{in}$$

The A_{in} could be a set of monoenergetic spectra or a set of isotopic spectra. Then the best least-squares fit would be obtained when

$$\sum_i W_i \left(\rho_i - \sum_n \beta_n A_{in}\right)^2 \equiv M$$

is a minimum. The W_i are weighting factors and the sum on i runs over all channels. The desired minimum is obtained by taking the partial derivative with respect to β_k for each of the m components

$$\frac{\partial M}{\partial \beta_k} = 2 \sum_i W_i \left(\rho_i - \sum_n \beta_n A_{in}\right) A_{ik} = 0$$

where

$$k = 1, 2, \ldots, m.$$

The matrix formulation of the last equation is[27]

$$A^T W_\rho - (A^T WA)\beta = 0$$

or

$$\beta = (A^T WA)^{-1} A^T W\rho$$

The usual weighting factor is $W_i = 1/\sigma_i^2 = \rho_i$.

Some difficulty has been encountered in obtaining a satisfactory fit of experimental data when the data contains peaks which have maxima that differ by several orders of magnitude, although quite satisfactory fits can be obtained with perfect data (as evidenced by fits of artificial spectra) even in such cases as just described. However, experimental data can be quite poor (low counting rates, etc.), and satisfactory fits not always obtained. Thus, the method just described is not universally applicable and an alternate procedure of treating the data has been provided.

The alternate method seems to yield an acceptable fit in the cases that the above method does not. The procedure is similar to the technique used in the qualitative analysis program, i.e. fitting a single peak at a time over a specified number of channels. Once the maximum energy peak is fitted in a least-squares sense, that peak and associated Compton distribution is subtracted from the experimental array, and the next peak is then analyzed. After the experimental spectrum has been analyzed (in either of the above two ways) to yield the normalized library spectra, the photopeak area of each library spectrum must be extracted. Each normalized library spectrum is summed, and this sum is then multiplied by the photofraction or peak to total ratio. The photofraction as a function of energy is a characteristic of the counting system; this curve has been shown

previously in Figure 5. This curve has been approximated by a polynomial, and the coefficients of the polynomials are stored in the computer program so that the photofraction for a particular energy can be computed rather than looked up in a table. The curve was broken up into two regions, and each fitted with a seventh order polynomial.

Corrections

If one wishes to perform absolute activity measurements, then there are certain corrections to the basic formula previously given. One of these corrections has already been discussed, i.e. the variation of detector efficiency with photon energy. When using the photopeak for activity calculations, the appropriate correction factor is the absolute photopeak efficiency ε_p. Recall also that as defined here, ε_p, contains the necessary geometric correction. The product $\phi\varepsilon_p A$, where ϕ represents the neutron flux, has been shown in Figure 7.

Another correction factor to be considered involves the decay scheme. As a simple example, consider the simplified decay scheme for ^{137}Cs shown in Figure 8. As can be seen from the decay scheme the 0.6616 MeV gamma-ray occurs in 93.5% of the transitions from ^{137}Cs to ^{137}Ba. Thus, the measured activity due to the gamma-ray alone must be divided by 0.935 to obtain the correct disintegration rate for ^{137}Cs. Let this factor be denoted by k_1. A comprehensive summary of decay schemes may be found in reference (28).

Another source of possible error is that due to absorption of radiation other than in the detector. This can occur in the source (self-absorption) and in materials near the source. The absolute

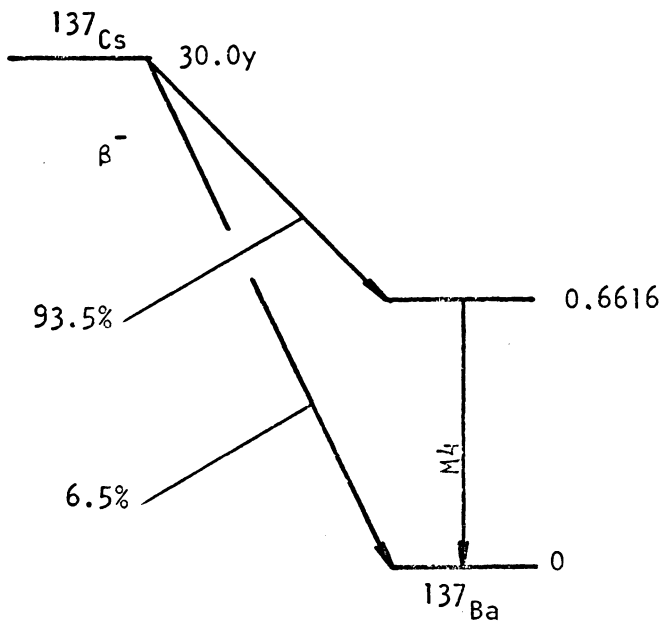

Figure 8. Decay Scheme of ^{137}Cs.

efficiency term corrects for absorption other than in the source. For photon energies above about 150 keV self-absorption errors are usually small[29]. Since in the present work the normal energy range considered is from about 200 keV to about 3100 keV, this correction factor is neglected. Of course, if the energy range is extended below 200 keV for a specific specimen, this correction factor will need to be considered. The size of the samples are kept as small as possible in order to reduce absorption in nearby materials.

A process which competes with photon emission as the means of nuclear de-excitation is that of internal conversion. The ratio of the number of conversion electrons to the number of photons emitted is defined to be the internal conversion coefficient. This coefficient is tabulated[30] as a function of atomic number, photon energy, electron shell, and type of photon transition. These tabulated coefficients allow one to apply the proper correction factor (k_2) to the measured activity. In general, internal conversion is more often important in heavy elements when relatively low energy (< 0.5 MeV) gamma-rays are emitted[31]. As an example, consider ^{137}Cs again. The proper correction factor is 0.945. That is, the measured activity should be divided by this number.

The measured counting rate must be extrapolated back to the time at which irradiation ended. This extrapolation factor is simply $e^{\lambda t'}$ where λ is the decay constant of the isotope and t' is the elapsed time between end of irradiation and the time at which the counting rate was measured. The latter time can be taken to the midpoint of the finite

counting interval when this interval is short compared with the half-life. When the counting interval is long compared to the half-life, the midpoint of the counting interval is no longer the proper time. A better estimate of this instant is that time at which the average activity (averaged over the counting interval) occurred. If this time is denoted as t', then the following result is readily obtained.

$$t' = t_1 + \frac{1}{\lambda} \ln [\lambda \Delta t (1 - e^{-\lambda \Delta t})^{-1}]$$

where t_1 is the instant at which the counting interval begins and Δt is the length of the interval. (This formulation is also used in the qualitative analysis in the calculation of half-lives).

The final correction to be considered is that for activation due to epithermal neutrons. The neutron activation cross-sections which are available (reference 34 is recommended for the most accurate values) are for thermal neutrons. However, the sample is also made radioactive with epithermal neutrons. Since the energy spectrum of the flux at the activation site does include epithermal neutrons, a correction must be applied. The energy dependence of the neutron flux in the V.P.I. reactor has been measured[35], but the correction applied here is based on measured activities. Cadmium has a large resonance in the neutron cross section at 0.175 eV[36], and when placed around a sample stops the thermal neutrons but is transparent to those neutrons of energy greater than about 0.4 eV[37]. Usually the cadmium cover is about 0.03 inches thick. Thus, if one activates a bare sample of a particular isotope and a cadmium covered sample, one can determine

from the resulting activities that part of the activity in the bare sample due to thermal neutrons. Let k_3 be defined as the ratio of the activity of the cadmium covered to the activity of the bare sample, then the correction to the activity of the uncovered sample (the normal method of activating samples in the present work) is $(1 - k_3)$. This correction is different for different isotopes, and depends, of course, on the resonance structure in the neutron cross section of each isotope.

When all these corrections are considered, the working relation for calculating the weight in grams of an isotope present is

$$w = \frac{W R e^{\lambda t'} (1 - k_3)}{(\phi \varepsilon_p A) A_o \sigma (1 - e^{-\lambda t}) k_1 k_2}$$

where

W = atomic weight of target nuclide

A_o = Avagadro's number

w = weight of target nuclide in grams,

and the remaining terms have been defined previously.

Test Case

In order to illustrate the use and capabilities of the programs just described, a test sample was activated, counted and analyzed. The sample consisted of sodium and indium, although this information was not used in the computer analysis prior to the comparison of the final output. While only two isotopes became radioactive upon neutron irradiation (^{24}Na and ^{116m}In), this sample provides a good test of the programs because of the large number of gamma-rays that are present. Sodium emits two gamma-rays with energies of 2.75 MeV and 1.368 MeV, and indium emits eight gamma-rays with energies of 2.08, 1.77, 1.49, 1.27, 1.085, 0.81, 0.406, and 0.137 MeV (the last of these is out of the normal energy range considered).

The data for this test case are shown in Figures 9, 10, 11, and 12. Figure 11 shows the original data for spectrum 5 and the computer fit to that data.

The open circles in Figure 11 are the original data for spectrum 5. The dashed curves are the shifted and normalized library spectra which the qualitative analysis program used in fitting the data, and the closed circles are the sum of the dashed curves. As can be seen from the figure a respectable fit to the rather complicated data was obtained even though eight components are present. The worst part of the fit occurs in the lower channels (20-65) as would be expected since this region has undergone six strippings by the time the analysis of the peaks in this region begins. The overall fit, however, is quite good. The area of the relatively poor fit will be discussed further, later in this section.

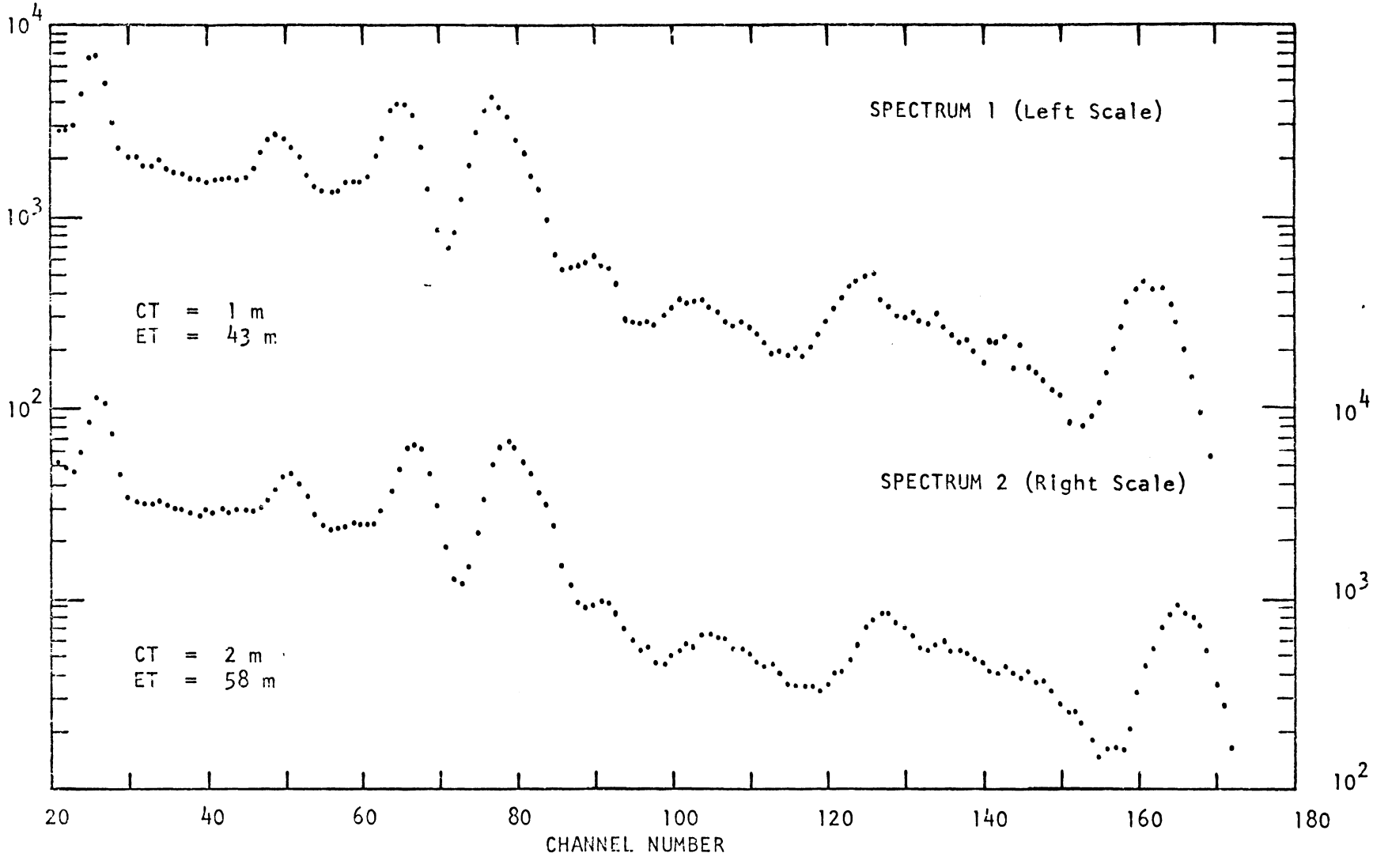

Figure 9. Data from Test Case.

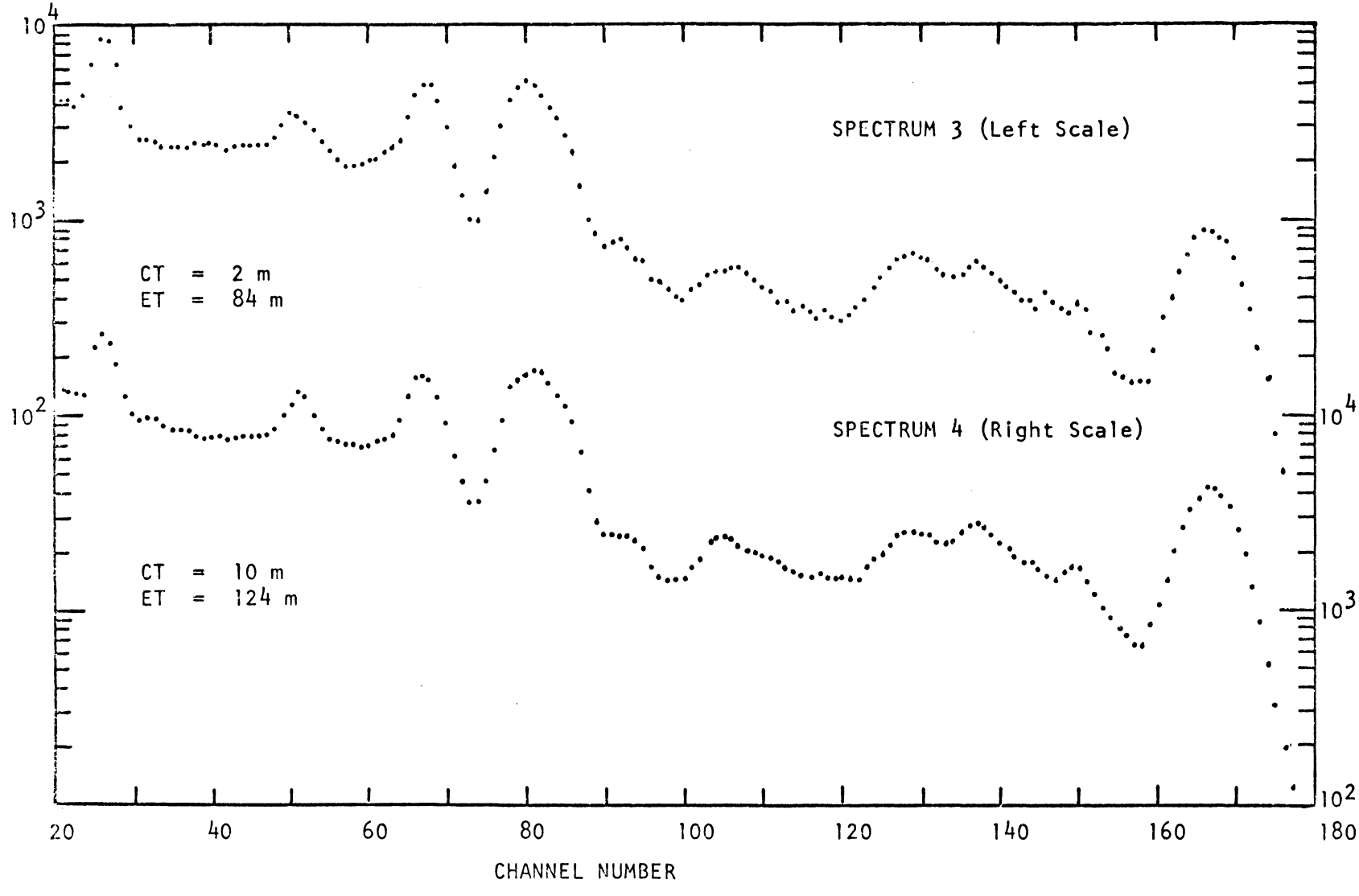

Figure 10. Data from Test Case.

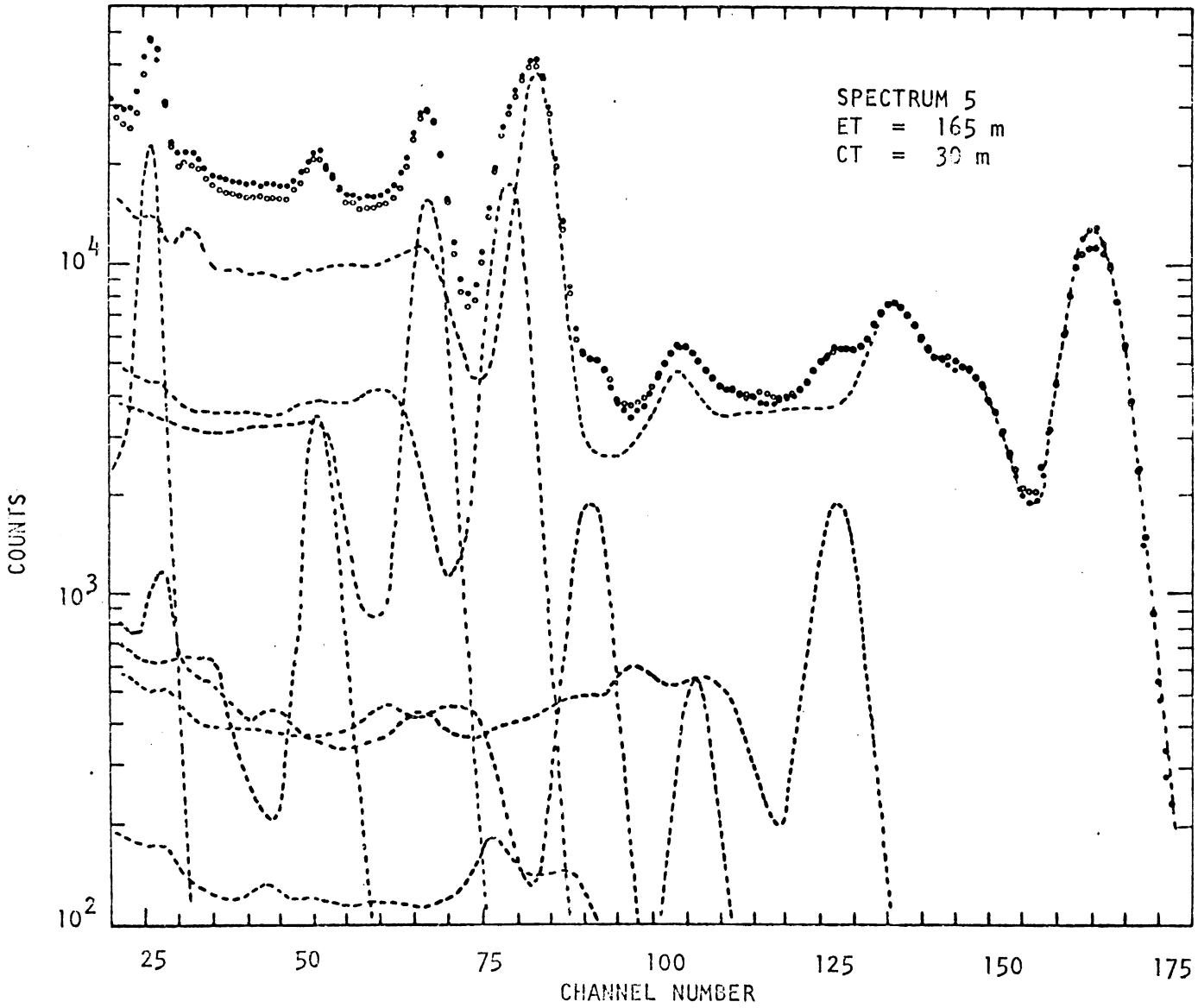

Figure 11. Data From Test Case Showing Components and Their Sum.

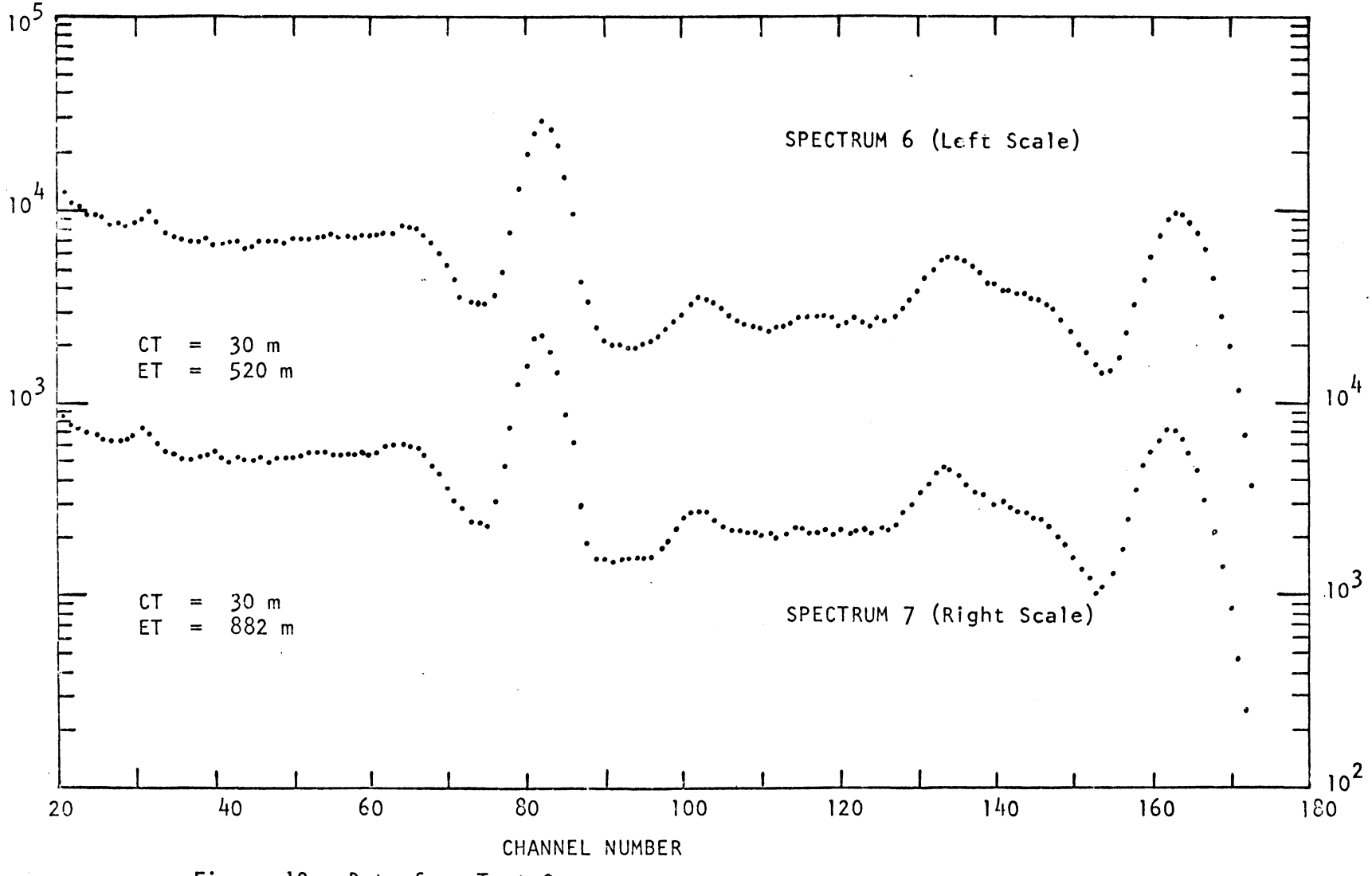

Figure 12. Data from Test Case.

The results of the qualitative computer program are shown in Table II. The half-lives shown are the averages as calculated by the computer and the intensity data are from spectrum 5. The data from this spectrum were chosen because the composite fit for spectrum 5 has been shown; however, similar results were obtained in the other spectra. No average value for the intensity is calculated as the program is now arranged, although the user can readily do this with the individual spectrum output. Although ^{24}Na emits two gamma-rays, the half-life for only one energy (2.75 MeV) is shown; this is because the isotopic spectrum of ^{24}Na is normally used. This spectrum is one of only two isotopic spectra in the library of gamma-rays. The isotopic spectra were chosen in these two cases because there are no other gamma-rays near the energies involved.

The calculated estimates of the half-lives are quite good as can be seen from the data in Table II. In all cases but one (the 0.81 MeV gamma-ray from ^{116m}In) the actual half-life lies within the calculated errors. The calculated relative intensities are quite good in these cases in which the relative intensity is high and the energy is greater than about 0.9 MeV. Below this energy an over-stripping (i.e. negative numbers left in the residual spectrum) occurred as was pointed out in the discussion of Figure 11. This over-stripping was due to a change in the counting geometry between the library data and the test case experiment. Although the source to detector geometry remained constant, a different physical situation existed nearby. This came about because the counter system is employed by others and a plastic scintillator

TABLE II

Isotope	Photopeak Energy (MeV)	Half-life		Relative Intensity	
		Actual	Computer	Actual	Computer
^{24}Na	2.75	15.0 h	(14.9 ± 1.6)h	-	-
^{116m}In	1.27	54.0 m	(52.5 ± 5.3)m	1.0	1.0
^{116m}In	1.09	54.0 m	(52.3 ± 4.2)m	0.65	0.68
^{116m}In	0.41	54.0 m	(52.4 ± 5.3)m	0.46	0.23
^{116m}In	2.08	54.0 m	(54.6 ± 3.5)m	0.24	0.25
^{116m}In	0.81	54.0 m	(49.0 ± 2.7)m	0.21	0.09
^{116m}In	1.49	54.0 m	(55.0 ± 5.8)m	0.14	0.15
^{116m}In	1.77	54.0 m	(53.4 ± 2.8)m	0.02	0.06

was substituted for the original second NaI(Tl) detector. Photofraction data showed that the result of this substitution resulted in significantly fewer Compton events due to scattered gammas from the second detector relative to the photopeak events. Thus since the 0.81 and 0.41 MeV gammas were superimposed upon the Compton distribution of the higher energy gammas, it is not surprising that the results obtained in these two cases would be affected. This over-stripping is the reason for the relative intensities of the 0.81 MeV and 0.41 MeV from ^{116m}In being low. The intensity for the 1.77 MeV indium gamma-ray is also not in good agreement with the true value. The relative intensity of this gamma-ray is quite low (0.02), and the computer was able to identify this photopeak in only two of the spectra. The relative intensities of gamma-rays in this range are quite difficult to measure accurately and the present result is not unreasonable.

From the data shown one would have no difficulty in assigning the proper isotopes present in the sample; this is the purpose of the qualitative analysis program.

In performing the quantitative analysis of the present case only one of the options previously described was exercised in determining the weight of Na and In. This one option was that of basing calculations on the activities calculated in the qualitative program. The other options were not used because the detector arrangement required for those options was not possible due to other demands on the counting system as previously stated.

The results of the quantitative analysis program are shown in Table III. The results are self-consistant within the discrepancies noted above. The actual mass of sodium present was 2.7 mg, and the mass of indium present was 10-20 μg. The experiment mass of indium cannot be assigned more accurately as the laboratory balance available is not sensitive enough for this range. The mass quoted above is based on the weighing of a larger sample which was divided and the fraction used was estimated on the ratio of the radioactivities using a simple survey meter for this measurement (not a part of the present programs). The calculated masses are very reasonable considering that the usual accuracy quoted for analysis based on absolute calibration is $\pm$ 20%[38].

Summary

The present program offers significant improvements in flexibility and accuracy over the previous qualitative program as demonstrated in the two tests cases discussed. In addition, a quantitative program has been added which affords good estimates on the amount of the unknown present. Improvement in this latter program could be achieved by accumulating a large amount of empirical data on specific radioisotopes and the specific detector equipment employed.

TABLE III

Element	Photopeak Energy (MeV)	Elemental Weight
^{24}Na	2.75	3.26 mg
^{116m}In	1.27	13.4 μg
^{116m}In	1.09	13.6 μg
^{116m}In	0.41	7.0 μg
^{116m}In	2.08	12.9 μg
^{116m}In	0.81	6.8 μg
^{116m}In	1.49	14.6 μg
^{116m}In	1.77	41.1 μg

APPENDIX

AIDS FOR IDENTIFICATION AND HAND CALCULATIONS:

Half-life Versus Energy:

All the (n,γ) reaction products that are shown in Heath's[32] catalog have been sorted by half-life. The results of this sorting are shown in Tables IV through XI . The listing of the radioactive products presented in this manner is useful in itself as an aid in identifying an unknown in a sample spectrum. However, the main purpose for this listing is to obtain the necessary information for plotting the half-life versus photon energy[33] for all the (n,γ) products shown in Heath.

Heath shows nearly 120 radioactive products produced by the (n,γ) reaction (and the majority of those have three or more gamma-rays). Since such a plot would only be useful if each point were labeled, the energy and half-life ranges were broken up into subdivisions, and a large number of page size graphs have been prepared. There is no correlation between the half-life and photon energy; the points on the plot are randomly distributed. For these reasons all the plots will not be shown here. However, a portion of one of them is shown in Figure 13 to illustrate the usefulness of this array.

As an example, consider one of the computer results from an early test case. A photopeak of 1.04 MeV decaying with a half-life of 5.2 minutes was found in the spectra of the test case. This was known to be the 1.04 MeV gamma-ray from ^{66}Cu which has a half-life of 5.1 minutes. Assuming the computer result did not match any of the known characteristics with which the experimenter was familiar, he

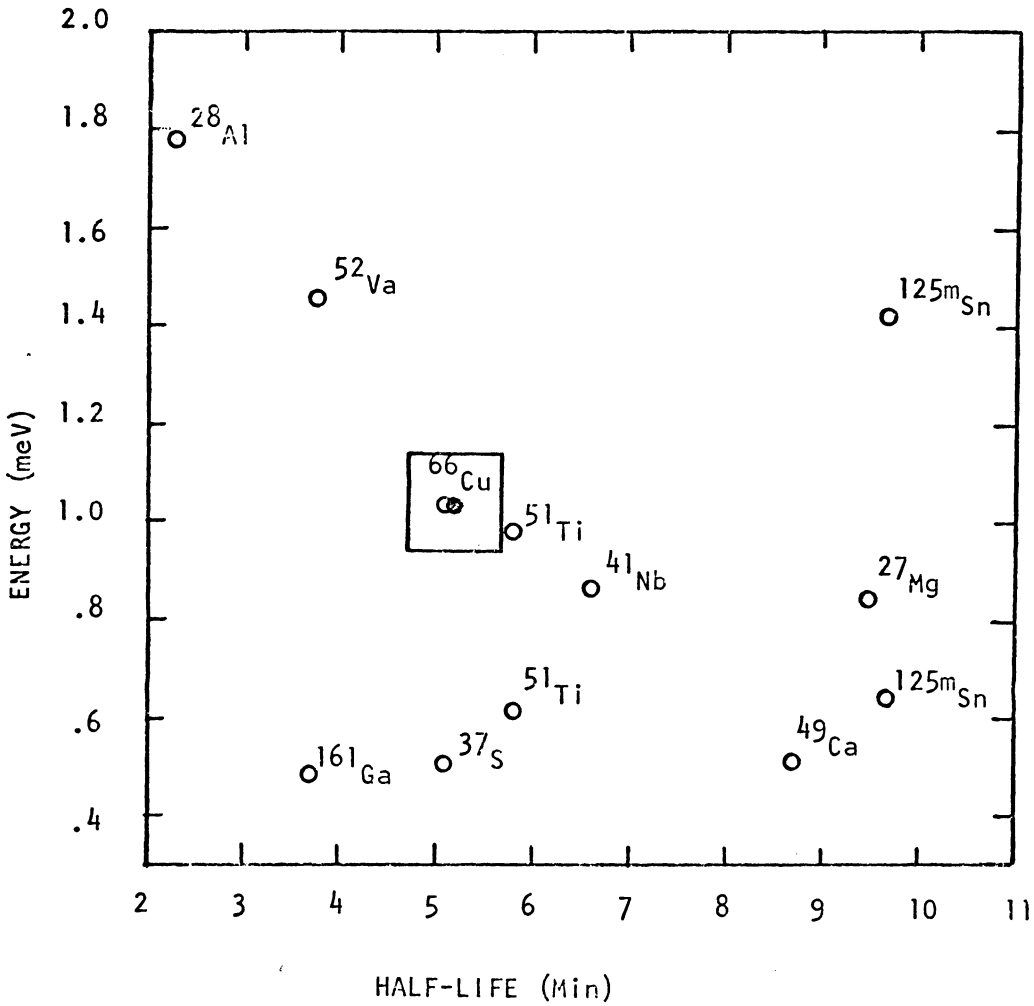

Figure 13. Example of the use of the Energy Versus Half-life Plots. The Open Circles are Points Given in Table V, the Closed Circle is an Experimental Point.

would proceed as follows. If the computed half-life and energy (closed circle in figure 13) are plotted, it is seen that the computed point nearly falls on the ^{66}Cu point. However, the ^{51}Ti point is not very distant from the computed point. If now the rectangle formed by the computed upper and lower limits of the half-life (5.8 minutes and 4.7 minutes, respectively) and the limits on the energy (0.94 MeV and 1.14 MeV) are drawn as shown in the figure, it is seen that only one possibility, ^{66}Cu, falls within the experimental error. Thus, a unique identification can be made. If more than one point had fallen within the rectangle, further criteria would be needed for unique identification (e.g., other gamma-rays with the same computed half-life, or the lack of other gamma-rays would probably enable the experimenter to make a unique identification).

As illustrated, the plot of half-life versus photon energy enables one to quickly eliminate all but a few possibilities or to uniquely make an identification. In those cases where an unstable isotope emits many gammas, only the most intense emissions are shown in the table (in order of decreasing intensity) and on the individual charts.

Nomograph

A nomograph which solves the equation

$$A = \sigma \phi (1 - e^{-\lambda t})$$

where

A = activity/mole of target nuclei

σ = neutron cross section

ϕ = neutron flux

λ = decay constant

and

t = activation time

has been prepared[37]. This nomograph is shown in figure 14.

The uses for this nomograph are two. First, it can be used for sensitivity calculations, i.e., if one wishes to know the minimum amount of a given isotope that can be detected. If the above equation is solved via the nomograph and if the efficiency of the counting system is known, one can judge what the lower limit of detection for a given isotope is. While the above equation is not difficult to solve, the nomograph eliminates the need to perform such hand calculations.

Another use of the nomograph is for rough quantitative results once the qualitative analysis has been done. Using the nomograph for calculating the specific activity (dps/mole) and the activity as calculated by the qualitative analysis program, one can compute the amount of the particular isotope present in the sample. Of course, the corrections to the computer calculated activity discussed previously should be made.

The nomograph is used as follows:

(1) Draw a line connecting the correct cross-section to the flux in which the sample is placed.

(2) Determine the number of half-lives over which the activation is done.

(3) Connect this last point with the point where the line in (1) crossed the α axis.

(4) Read the activity (dps/mole) from the A axis where the line in (3) crossed.

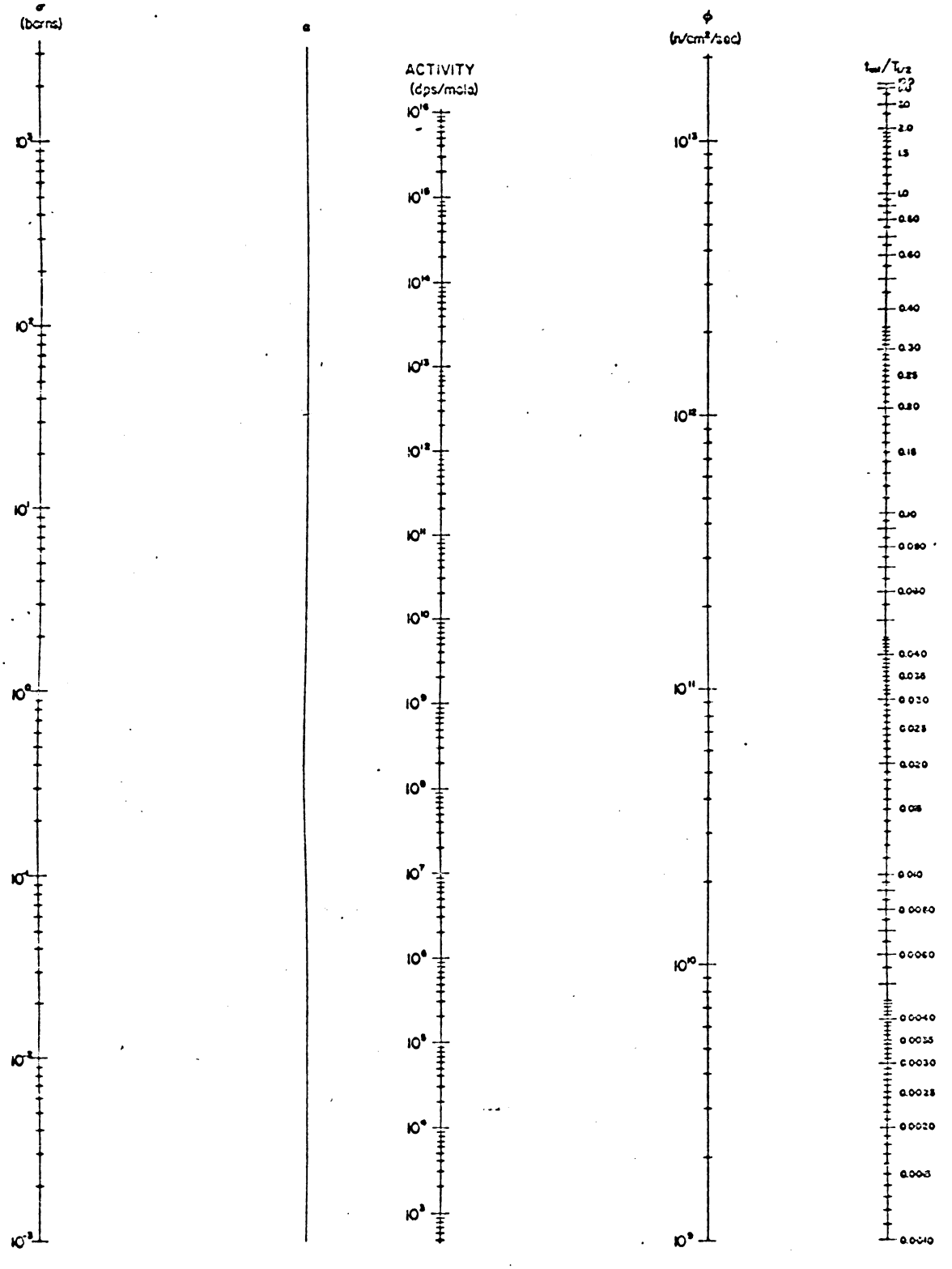

Figure 14. A nomograph for solving the equation $A = N\sigma(1 - e^{-\lambda t})$

TABLE IV

Element	Isotope	Half-life (sec.)	Energy (MeV)
Hafnium	179m	19	.215, (.16)
Silver	110	24	.656, (B)
Rhodium	104	42	.555
Germanium	77m	54	.215

TABLE V

Element	Isotope	Half-life (min.)	Energy (MeV)
Dysprosium	165m	1.25	.515, .361, (.155)
Aluminum	28	2.3	1.78
Silver	108	2.4	.633, .511, .433, (.509, .433, .615, B)
Antimony	122m	3.4	.075, .061, (.027X)
Gadolinium	161	3.7	.485, .363, .316, (.28, .18, +)
Vanadium	52	3.77	1.43
Rhodium	104m	4.4	.10, .077, (.051)
Copper	66	5.1	1.04, (B)
Sulfur	37	5.1	3.13, .511
Titanium	51	5.8	.94, .62, .322
Niobium	94m	6.6	.871
Calcium	49	8.7	3.09, .511, 4.05, (4.7)
Magnesium	27	9.5	.842, 1.01, (.168)
Tin	125m	9.7	.331, .593, .65, 1.42, (1.04, .85)

TABLE VI

Element	Isotope	Half-life (min.)	Energy (MeV)
Cobalt	60m	10.5	1.33, (.059)
Neodymium	151	12	.115, .17, .254, 1.08, (+)
Molybdenum	101	14.6	.193, .592, (+)
Tantalum	182m	16	.172, .184, .146, .318, (.057)
Bromine	80	18	.612, .665, .511, (B)
Rubidium	88	18	1.04, .665, 1.256, 2.21 (+)
Selenium	81	18	.28
Rhenium	188m	18.7	.106, .092, (.06X)
Gallium	70	21	.17, 1.04, (B)
Uranium	239	23.5	.074, (+)
Iodine	128	25	.445, (+, B)
Samarium	155	25	.106, .142, .245
Platinum	199	30	.189, .540, (+)
Chlorine	38	38	1.64, 2.16, .511
Indium	116m	54	.406, 1.085, 1.27, (+)
Selenium	81m	61	.103
Lead	204m	67	.375, .899, (.912)
Germanium	75	82	.266, .199, (+)
Barium	139	83	.166, 1.43, (B)

TABLE VII

Element	Isotope	Half-life (hours)	Energy (MeV)
Argon	41	1.83	1.27
Neodymium	149	1.9	.112, .198, (+)
Dysprosium	165	2.3	.361, .277, (+)
Manganese	56	2.58	.845, 1.81, 2.12
Silicon	31	2.62	1.27, (B)
Nickel	65	2.65	.37, 1.114, 1.48, (+)
Strontium	87m	2.8	.391
Cesium	134m	2.9	.127
Lutetium	176m	3.7	.0883, (B)
Krypton	85m	4.4	.305, .150
Ruthenium	105	4.45	.723, .472, .316, (+)
Hafnium	180m	5.5	.216, .333, .444, (+)
Erbium	171	7.5	.308, .296, .117, (+)
Europium	152m	9.3	.122, .344, .841, .963, (+)

TABLE VIII

Element	Isotope	Half-life (hours)	Energy (MeV)
Germanium	77	11	.215, .264, .416, .561, (+)
Potassium	42	12.4	1.52, .3, (B)
Copper	64	12.8	.511, 1.34
Palladium	109	13.6	.088, (B)
Zinc	69m	14	.44
Gallium	72	14.1	.81, .62, 2.2, 2.5, (+)
Sodium	24	15	1.368, 2.75
Rhenium	188	17	.155, .478, .633, (+)
Zirconium	97	17	.25, .35, .51, 1.15, (+)
Gadolinium	159	18	.362, .305, .225
Xenon	125	18	.1876, .243, .46, (+)
Iridium	194	19	.328, .645, .939, (+)
Praseodymium	142	19.2	1.58, (B)
Platinum	197	20	.191, .269
Magnesium	28	21.3	.40, .95, 1.35
Mercury	197m	24	.135, .278
Tungsten	187	24	.134, .480, .686, (+)
Arsenic	76	26.5	.559, .657, 1.22, (+)
Osmium	193	32	.139, .281, .460, .559, (+)
Cerium	143	35	.294, .232, .351, (+)
Bromine	82	36	.554, .777, 1.044, 1.317, (+)
Lanthanum	140	40.2	.487, .327, .868, 1.597, (+)
Samarium	153	46.7	.103, .0697

TABLE IX

Element	Isotope	Half-life (days)	Energy (MeV)
Gold	198	2.7	.412, .076, 1.089
Mercury	197	2.7	.191, .269
Molybdenum	99	2.75	.181, .372, .74, .78
Cadmium	115	2.3	.26, .523, (+)
Antimony	122	2.8	.561, .687, (1.13, 1.24)
Ruthenium	97	2.9	.215, .323, .565
Platinum	195m	4.1	.099, .130
Ytterbrium	175	4.2	.1138, .283, .396, (+)
Tantalum	183	5.2	.1, .161, .244, (+)
Lutetium	177	6.8	.113, .208, (.25)
Neodymium	147	11.1	.091, .32, .54, (+)
Barium	131	11.5	.126, .220, .498, (+)
Osmium	191	15	.129
Rubidium	86	18.7	1.077, (B)
Chromium	51	27.8	.322

TABLE X

Element	Isotope	Half-life (days)	Energy (MeV)
Ytterbrium	169	32	.110, .177, .308, (+)
Cerium	141	32.5	.145
Ruthenium	103	40	.498, .611, .297, (.053)
Cadmium	115m	43	.935, .485, 1.295, (1.13)
Hafnium	181	43	.482, .346, .136
Iron	59	45	1.097, 1.289, .191, (.145, .337)
Mercury	203	47	.279
Indium	114m	49	.192, .556, .722, (1.3)
Tellurium	125m	58	.110
Antimony	124	60	.603, .722, 1.69, (+)
Hafnium	175	70	.343, (+)
Terbium	160	73	.298, .216, .879, .962, (+)
Iridium	192	74	.3165, .468, .613, (+)
Scandium	46	85	.887, 1.119
Osmium	185	94	.646, .879, (+)
Tantalum	182	115	1.12, 1.22, (+)
Tin	113	118	.253
Selenium	75	120	.136, .265, .402, (+)
Thulium	170	127	.084, (B)
Gadolinium	153	200	.1032, .0697
Zinc	65	245	1.114, .511
Silver	110m	250	.71, .885, 1.384, (+)

TABLE XI

Element	Isotope	Half-life (year)	Energy (MeV)
Cadmium	109	1.29	.088
Cesium	134	2.1	.605, .801, (+)
Cobalt	60	5.27	1.1173, 1.332
Barium	133	7.5	.08, .355, (+)
Krypton	85	10.4	.515, (B)
Niobium	94	2×10^4	.702, .871

REFERENCES

1. Guinn, Vincent P., Neutron Activation Analysis with Research Reactors, Transactions of American Nuclear Society, Volume 9, Number 2, p. 588, (Oct.-Nov., 1966).

2. Corliss, William R., Neutron Activation Analysis, U. S. Atomic Energy Commission, Division of Technical Information, p. 10, (1964).

3. Guinn, Vincent P., "Forensic Applications of Activation Analysis", in Activation Analysis, Proceedings of a NATO Advanced Study Institute held in Glasgow, Lenihan, J.M.A., and Thomson, S. J., editors, pp. 125-127, Academic Press, New York, (1965).

4. Wood, Donald E., "Activation Analysis in the Metals Industry", Nuclear News, Volume 9, Number 9, pp. 12-17, (Sept., 1966).

5. Hevesg, G., and Levi, H., Danske Videnskab, Selskab Mathfys. Medd. 14 (5), 1937.

6. Lyon, William S., editor, Guide to Activation Analysis, D. Van Nostrand Company, Inc., Princeton, N. J., (1964).

7. Taylor, Denis, Neutron Irradiation and Activation Analysis, D. Van Nostrand Company, Inc., Princeton, N. J., (1964).

8. Koch, Robert C., Activation Analysis Handbook, Academic Press, New York, (1960).

9. Raleigh, Henry D., Activation Analysis: A Literature Search (TID-3575), (August, 1963).

10. Wood, Donald E., Selected References for Neutron Activation Analysis, Technical Bulletin #108, Kaman Nuclear Publication, April, 1968.

11. Siegbahn, Kai, editor, Alpha-, Beta-, and Gamma-Ray Spectroscopy, Volume I, Chapter VIII, Part (B), North-Holland Publishing Company, Amsterdam, (1965).

12. Haller, William A., Raneitelli, Louis A., Cooper, John A., "Instrumental Determination of Trace Elements in Plant Tissue by Neutron Activation Analysis and Ge(Li) Gamma-Ray Spectrometry", Journal of Agricultural and Food Chemistry, 16, 1036-40 (Nov. - Dec. 1968).

13. (STI/PUB-155) Nuclear Activation Techniques in the Life Sciences, Proceedings of the Symposium held in Amsterdam, International A.E.A., Vienna (Austria), (1967).

14. Lomard, S. M., and Isenhom, T. L., "Neutron Capture Gamma-Ray Activation Analysis Using Lithium Drifted Germanium Semiconductor Detectors", Analytical Chemistry, 40; 1990-4, (Nov. 1968).

15. Lyon, William S., Guide to Activation Analysis, D. Van Nostrand Company, Inc., Princeton, N. J., pp. 109-110, (1964).

16. Strain, J. E., "Use of Neutron Generators in Activation Analysis", Progress in Nuclear Energy, Series IX, Volume 4, Part 3, Pergamon Press, (1965).

17. Guinn, V. P., Graber, F. M., and Fleishman, D. M., "Ge(Li) Gamma-Ray Spectrometry as a Pilot for NaI(Tl) Gamma-Ray Spectrometry", Talanta, Vol. 15, 1159-1163, (1968).

18. Heath, R. L., "Scintillation Spectrometry Gamma-Ray Spectrum Catalogue", 2nd Ed., 1, 2, AEC Research and Development Report IDO-16880-1, (August, 1964).

19. Winters, R. R., "Half-life Determination of Lutetium-176 by Three Coincidence Methods", VPI Ph.D. Dissertation, unpublished (1967).

20. Robins, C. H., "A Digital Computer Technique for Qualitative Analysis of Complex Samples from Their Neutron Induced Gamma-Ray Activities", Ph.D. Dissertation, Virginia Polytechnic Institute, Blacksburg, Virginia, 1966, (unpublished).

21. Robinson, E. L., "An Examination of the Operating Characteristics of the V.P.I. Neutron Activation Analysis Program", Masters Thesis, Virginia Polytechnic Institute, 1967 (unpublished).

22. Furr, A. K., Robinson, E. L., and Robins, C. H., "A Spectrum Stripping Technique for Qualitative Activation Analysis Using Monoenergetic Gamma Spectra", Nuclear Instruments and Methods, 63, 205-209, (1968).

23. Siegbahn, Kai, editor, Alpha-, Beta-, and Gamma-Ray Spectroscopy, Vol. 1, p. 528, North-Holland Publishing Company, Amsterdam, (1965).

24. Ibid, p. 529.

25. R. L. Heath, Scintillation Spectrometry, AEC Document, IDO-16880-1, Vol. 1, Appendix II, (1964).

26. Trombka, J. I., "Least-Squares Analysis of Gamma-Ray Pulse-Height Spectra", Applications of Computers to Nuclear and Radiochemistry, G. D. O'Kelley, ed., Proceedings of a Symposium, NAS-NS 3107, (1962).

27. Rose, M. E., "The Analysis of Angular Correlation Distribution Data", Physical Review, 91, 610 (1953).

28. Lederer, C. M., Hollander, J. M., and Perlman, I., Table of Isotopes, Sixth Edition, John Wiley and Sons, New York, (1968).

29. Taylor, Denis, Neutron Irradiation and Activation Analysis, D. Van Nostrand Company, Inc., Princeton, p. 181, (1964).

30. Siegbahn, K., editor, Alpha-, Beta-, and Gamma-Ray Spectroscopy, Appendix 5, North-Holland, Amsterdam, (1966).

31. Kaplan, I., Nuclear Physics, Second Edition, Addison-Wesley, Reading, Mass., p. 428, (1963).

32. Heath, R. L., Scintillation Spectrometry, AEC Document, IDO-16880-1, Volume II, (1964).

33. Ljmggren, K., and Westermark, T., "A Method for the Detection of Mercury by Radioactivation Analysis", Proceedings of the Radioactivation Analysis Symposium held in Vienna, (June, 1959).

34. Goldberg, M. D., Mughabghab, S. F., Magurano, B. A., and May, V. M., Neutron Cross Sections, Volumes I-V, BNL 325, (February, 1966).

35. Furr, A. K., and Tucker, J. R., "Average s- and p-Wave Resonance Parameters of ^{115}In and ^{127}I", Nuclear Science and Engineering, Vol. 35, 364-370, (1969).

36. Hughes, D. J., and Harvey, J. A., Neutron Cross Sections, BNL 325, (July, 1955).

37. Campbell, W. W., Private Communication.

38. Lyon, William S., op. cit., p. 9.

The vita has been removed from the scanned document

NEUTRON ACTIVATION ANALYSIS USING MONOENERGETIC GAMMA-RAY SPECTRA

E. Larry Robinson

ABSTRACT

Computer programs for performing both qualitative and quantitative neutron activation analysis using monoenergetic gamma-ray spectra have been developed. The qualitative analysis is based on the spectrum stripping technique. The quantitative analysis is based primarily on the absolute calibration of the counting system; however, the comparator technique can be used with the present program. The methods used are described and a test case is presented to illustrate the use and capability of the programs.